

## On the Mechanism of Nonspecific Inhibitors of Protein Aggregation: Dissecting the Interactions of $\alpha$ -Synuclein with Congo Red and Lacmoid<sup>†</sup>

Christofer Lendel,<sup>‡,⊥</sup> Carlos W. Bertocini,<sup>‡,⊥</sup> Nunilo Cremades,<sup>‡</sup> Christopher A. Waudby,<sup>‡</sup> Michele Vendruscolo,<sup>‡</sup> Christopher M. Dobson,<sup>\*,‡</sup> Dale Schenk,<sup>§</sup> John Christodoulou,<sup>‡,||</sup> and Gergely Toth<sup>\*,§</sup>

<sup>‡</sup>Department of Chemistry, University of Cambridge, Lensfield Road, Cambridge CB2 1EW, U.K., <sup>§</sup>Elan Pharmaceuticals, 700 Gateway Boulevard, South San Francisco, California 94080, and <sup>||</sup>Department of Structural & Molecular Biology, University College London, Gower Street, London WC1E 6BT, U.K. <sup>⊥</sup>C.L. and C.W.B. contributed equally to this work

Received July 26, 2009

**ABSTRACT:** Increasing evidence links the misfolding and aberrant self-assembly of proteins with the molecular events that underlie a range of neurodegenerative diseases, yet the mechanistical details of these processes are still poorly understood. The fact that many of these proteins are intrinsically unstructured makes it particularly challenging to develop strategies for discovering small molecule inhibitors of their aggregation. We present here a broad biophysical approach that enables us to characterize the mechanisms of interaction between  $\alpha$ -synuclein, a protein whose aggregation is closely connected with Parkinson's disease, and two small molecules, Congo red and Lacmoid, which inhibit its fibrillization. Both compounds are found to interact with the N-terminal and central regions of the monomeric protein although with different binding mechanisms and affinities. The differences can be attributed to the chemical nature of the compounds as well as their abilities to self-associate. We further show that  $\alpha$ -synuclein binding and aggregation inhibition are mediated by small oligomeric species of the compounds that interact with distinct regions of the monomeric protein. These findings provide potential explanations of the nonspecific anti-amyloid effect observed for these compounds as well as important mechanistical information for future drug discovery efforts targeting the misfolding and aggregation of intrinsically unstructured proteins.

A number of severe disorders, including Alzheimer's, Parkinson's (PD) and prion diseases and frontotemporal dementia are linked to protein misfolding and aggregation (1). The mechanisms by which proteins of wide structural diversity are transformed into morphologically similar aggregates seem to be a generic property of the peptide backbone (1). Structural transformations into fibrillar assemblies have been observed for a range of globular proteins and in particular from intrinsically unstructured polypeptides, including the amyloid  $\beta$  (A $\beta$ ) peptide, microtubule-associated protein tau and  $\alpha$ -synuclein ( $\alpha$ S) (2).

The growing class of protein misfolding diseases provides a significant opportunity and a challenge for drug discovery. Though a large number of small molecules have been shown to inhibit fibril formation *in vitro*, the details of their mechanisms of action are often poorly understood. Presently, no approved therapeutic agent that blocks the formation of amyloid structures exists. The fact that many protein aggregation inhibitors are reported to act on several amyloidogenic proteins (3) certainly raises questions about their specificity. Furthermore, different inhibitors seem to affect different steps along the fibril formation pathway, as recently illustrated for A $\beta$  by Necula and co-workers (4). However, the lack of understanding of the degree of

cytotoxicity of the various protein species populated along the aggregation pathways (5) suggests that an effective therapeutic strategy should maintain the proteins in their native states and thus hinder the formation of all oligomeric and prefibrillar species. In the case of globular proteins, partial unfolding has been found to trigger aggregation and, therefore, stabilization of the globular fold would provide a possible avenue for aggregation inhibition (1). In cases where the amyloidogenic precursors are intrinsically unstructured proteins, the approach for stabilizing the native state by a small molecule binder is less obvious.

Interestingly, some small molecules, for example, Congo red (CR, Figure 1a), Lacmoid (Lac, Figure 1b) and the polyphenol EGCG (6), have recently been reported to affect fibril formation of several amyloidogenic proteins, including  $\alpha$ S and A $\beta$  (3, 4) and to interact with the monomeric intrinsically unstructured proteins (6, 7). Such compounds thus represent exceptionally interesting model systems for characterizing the nature of protein binding and aggregation inhibition mechanisms. Lac, similarly to EGCG, contains polyphenol groups and resembles a class of compounds called phenothiazines that serves as a scaffold for several neuroleptic antipsychotic drugs such as Thorazine, Prolixin and perphenazine. CR is a histological dye frequently used to detect the presence of amyloid fibrils through a shift in absorption spectrum, induced fluorescence and the display of yellow-green birefringence under cross-polarized light (8). CR is reported to interact with a number of structured and unstructured proteins and to interfere with protein misfolding and aggregation processes (3, 9, 10). The details of the mechanism by which CR binds to proteins are not well understood, and substantial discrepancies exist in the reported effects on protein

<sup>†</sup>This work was supported by EMBO (C.L. and C.W.B.), the Swedish Research Council (C.L.), and the Leverhulme and Wellcome trusts.

\*To whom correspondence should be addressed. C.M.D.: Department of Chemistry, University of Cambridge, Lensfield Road, Cambridge CB2 1EW, U.K. Phone: +44-1223-763070. Fax: +44-1223-763418. E-mail: cmd44@cam.ac.uk. G.T.: Elan Pharmaceuticals, 700 Gateway Boulevard, South San Francisco, CA 94080. Phone: 650-714-5335. Fax: 650-877-7486. E-mail: Gergely.Toth@gmail.com.

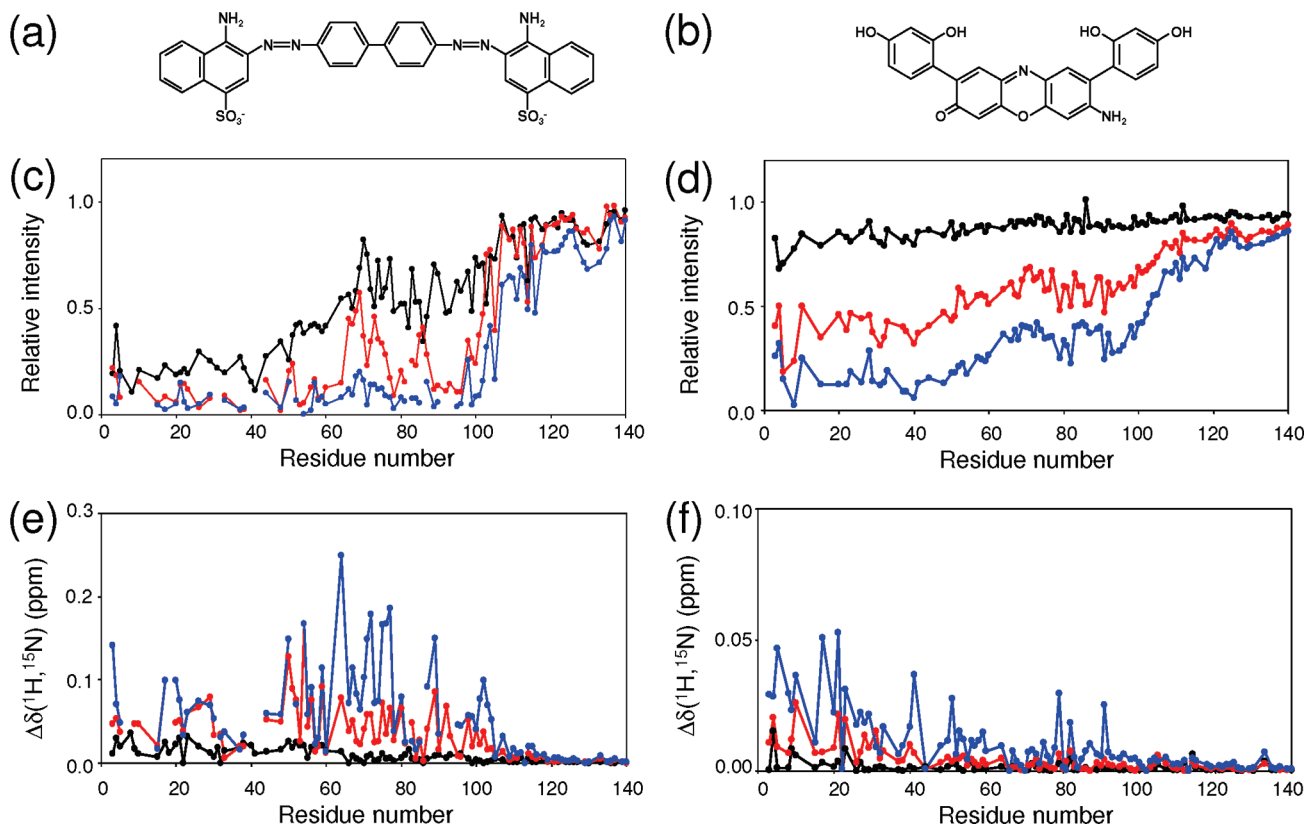


FIGURE 1: Heteronuclear NMR shows that CR and Lac interact differently with the N-terminal and NAC regions of  $\alpha$ S. Chemical structures of CR (a) and Lac (b). Changes in intensities (c, d) and chemical shifts (e, f) of resonances in the  $\alpha$ S  $^1\text{H}$ - $^{15}\text{N}$  HSQC spectrum due to addition of CR or Lac. (c, e) 100  $\mu\text{M}$   $\alpha$ S with 2:1 (black), 5:1 (red) and 10:1 (blue) molar excess of CR. (d, f) 100  $\mu\text{M}$   $\alpha$ S with 1:1 (black), 6:1 (red) and 16:1 (blue) molar excess of Lac. The reported chemical shifts changes are weighted averages of the  $^1\text{H}$  and  $^{15}\text{N}$  chemical shift changes  $[(\Delta\delta(^1\text{H}))^2 + (\Delta\delta(^{15}\text{N})/5)^2]^{1/2}$ .

aggregation (8). Such discrepancies could be related to the ability of the dye to self-associate into micelle-like species (11–13) which is a behavior that appears to be characteristic of many nonspecific (promiscuous) inhibitors (14) frequently encountered among “hits” originating from high-throughput drug discovery screening. In fact, a recent report suggests that the ability of self-assembly may be a general property of small molecule inhibitors of amyloid fibril formation and that the formation of large colloidal particles is mechanistically linked to the inhibition of protein aggregation (15). Such an effect could indeed be related to the broad anti-amyloid effect observed for many small molecules and increased understanding of the inhibition mechanisms of these compounds would provide important information when designing approaches for drug development targeting aggregation-related diseases.

Formation of intracellular aggregates containing the presynaptic protein  $\alpha$ S is the hallmark of a group of neurodegenerative disorders called  $\alpha$ -synucleinopathies, with the most well-known variant being PD (16).  $\alpha$ S is a 14 kDa intrinsically unstructured protein whose normal function is not yet well understood, but its overexpression and aggregation is a pathological event associated with Lewy bodies and neuritis, a hallmark of this group of neurodegenerative disorders (17). Characterization of the conformational properties of  $\alpha$ S using NMR spectroscopy has revealed the presence of both local and long-range interactions within the fluctuating structural ensemble (18–20). Many aggregation promoting conditions, including high ionic strength, low pH or the presence of polyamines, have been shown to be accompanied by structural changes in the protein (20, 21) suggesting that the observed long-range interactions are

fundamental for the definition of the native state of the protein and may provide an opportunity for the stabilization of protective native-like interactions and impair amyloid aggregation. In addition, the protein exist in a lipid-bound state in which the  $\alpha$ -helical content is dramatically increased (18, 22, 23).

Rao and co-workers recently investigated the interaction between monomeric  $\alpha$ S and selected small molecules, including Lac and CR, using NMR and CD spectroscopy (7). However, neither the details of the protein aggregation inhibition mechanisms nor the impact of the self-association of the small molecules on the binding affinity and specificity were addressed. Such characterization is crucial to fully understand the way the investigated inhibitors modulate protein aggregation. In this study, that was conducted in parallel and independently of the work reported by Rao and collaborators, we attempt to dissect the mechanisms by which Lac and CR interact with monomeric  $\alpha$ S. We combine residue-specific NMR data with a wide range of complementary biophysical techniques to link the protein:ligand interactions to the inhibition of protein aggregation. Moreover, we investigate the key role that the self-association capabilities of the small molecule compounds play in their anti-amyloid activities.

## EXPERIMENTAL PROCEDURES

**Materials.**  $\alpha$ S was expressed in *Escherichia coli* BL21 cells using a pT7-7 vector as described in ref 24.  $^{15}\text{N}$ - and  $^{13}\text{C}$ - $^{15}\text{N}$ -labeled protein was produced using M9 minimal medium supplemented with  $^{15}\text{NH}_4\text{Cl}$  and  $^{13}\text{C}$ -glucose (Cambridge Isotope Labs). The protein was purified using heat treatment, ammonium sulfate precipitation, anion exchange and size exclusion chromatography as previously described (24). Purified protein samples

were dialyzed against water, flash frozen in liquid nitrogen and stored at  $-80^{\circ}\text{C}$ . Production of A24C and Q62C  $\alpha\text{S}$  mutants has been reported elsewhere (19). Labeling with the fluorescent dye IAEDANS (Sigma) was performed following standard protocols. Briefly, 1 mg of purified cysteine-containing protein was reduced by incubation in 10 mM DTT for 30 min. The reducing agent was removed by fast desalting in PD-10 columns (GE healthcare) and a 10:1 molar excess of the dye was immediately added. Proteins were incubated with the dye for 1 h at  $4^{\circ}\text{C}$ , and the excess of fluorophore was removed with another fast desalting step in PD-10 columns. The yield of labeling reached 99%. Lac and CR were dissolved in buffer to prepare stock solutions of 1–50 mM. These solutions were sonicated before further dilution. Purified fraction V albumin from bovine serum (BSA, Sigma) was employed without further purification.

**NMR Spectroscopy.** NMR samples were prepared in 25 mM Tris buffer pH 7.4 with 100 mM NaCl and 10%  $^2\text{H}_2\text{O}$  if nothing else is stated. Data were recorded on Bruker Avance 400 MHz, 500 MHz, and 700 MHz spectrometers (the latter two equipped with cryoprobes), processed using NMRPIPE (25) or TopSpin (Bruker) and analyzed in CCPNMR (26), TopSpin (Bruker) or Sparky (T. D. Goddard and D. G. Kneller, SPARKY 3, University of California, San Francisco, CA). All NMR experiments, except for the diffusion measurements, were performed at  $10^{\circ}\text{C}$ , to avoid the enhanced line broadening at higher temperatures (27).

2D  $^1\text{H}$ – $^{15}\text{N}$  heteronuclear single quantum correlation (HSQC) (28) spectra were recorded with  $512 \times 128$  complex points and spectral widths of  $10 \times 29.5$  ppm. The HSQC spectrum of  $100\ \mu\text{M}$   $\alpha\text{S}$  was monitored during addition of 0.5 to 16 and 1 to 10 molar equiv of Lac and CR respectively. Assignment of the  $^1\text{H}$ – $^{15}\text{N}$  correlation spectrum of free  $\alpha\text{S}$  has previously been reported (18, 29). The assignments of the  $\alpha\text{S}$  spectra in the presence of Lac or CR were done by following the peaks in the correlation map during the titration.

2D  $^1\text{H}$ – $^{15}\text{N}$  correlation spectra of  $1\ \mu\text{M}$   $\alpha\text{S}$  with and without  $4\ \mu\text{M}$  CR were recorded using SOFAST-HMQC (30) with  $512 \times 64$  complex points,  $12 \times 29$  ppm spectral widths and 1,152 or 1,280 scans per increment.

$^{13}\text{CO}$ – $^{15}\text{N}$  correlation spectra were recorded with direct  $^{13}\text{C}$  detection (31, 32) using the 500 MHz spectrometer equipped with a TCI probe (Bruker).  $512 \times 256$  complex points were recorded with spectral widths of  $10 \times 40$  ppm (to include Pro residues) and with 16 scans per increment. Two spectra were collected and added to reduce noise. Samples contained  $100\ \mu\text{M}$   $^{13}\text{C}^{15}\text{N}$ -labeled  $\alpha\text{S}$  with the addition of 0.9 mM CR or 0.6 mM Lac.

Pulsed field gradient (PFG) NMR experiments were acquired at  $15^{\circ}\text{C}$  on the 700 MHz spectrometer using a  $100\ \mu\text{M}$  unlabeled protein sample in 50 mM phosphate buffer (pH 7.6) (uncorrected), 100 mM NaCl, in 99.9%  $^2\text{H}_2\text{O}$  and containing 10 mM dioxane as an internal radius standard and viscosity probe (33). 24 1D  $^1\text{H}$  spectra were collected as a function of gradient strengths from  $1.60\ \text{G cm}^{-1}$  to  $32.0\ \text{G cm}^{-1}$ , in a linear manner. Each  $^1\text{H}$  spectrum comprised 32 scans (or 128 scans in the case of CR). 8,192 complex points were acquired with a spectral width of 12 ppm. The dioxane peak and selected signals in the aromatic and aliphatic regions of the  $^1\text{H}$  protein spectrum were integrated and the decay of the signals as a function of the gradient strength was fitted to a Gaussian function using Sigma plot 7.0 to determine the hydrodynamic radii (33). The radius of hydration for the protein ( $R_{\text{H,prot}}$ ) was calculated from the decay rates of the protein and the dioxane peaks, using the formula  $R_{\text{H,prot}} =$

$(d_{\text{diox}}/d_{\text{prot}})R_{\text{H,diox}}$ , whereas  $R_{\text{H,diox}}$  is  $2.12\ \text{\AA}$ , and  $d_{\text{diox}}$  and  $d_{\text{prot}}$  are the dioxane and protein decay rates, respectively.

1D NMR spectrum of Lac were recorded at 400 MHz  $^1\text{H}$  frequency at  $25^{\circ}\text{C}$ . The sample contained 0.5 mM Lacmoid in 25 mM Tris buffer pH 7.4 with 100 mM NaCl. 512 scans were added in the final spectrum.

**Fluorescence Spectroscopy.** The binding affinities of the  $\alpha\text{S}$ : ligand complexes were determined from fluorescent quenching of  $5\ \mu\text{M}$  IAEDANS conjugated  $\alpha\text{S}$  ( $\alpha\text{S}$ -62C-AEDANS for CR and  $\alpha\text{S}$ -24C-AEDANS for Lac) when titrated with  $1\ \mu\text{M}$  to 0.5 mM CR or Lac. The experiments were performed in 25 mM Tris buffer pH 7.4, 100 mM NaCl, using a Cary-Eclipse spectrofluorimeter (Varian). An excitation wavelength of 337 nm was used and the emission was measured from 400 to 600 nm. The decrease in fluorescence intensity at 480–520 nm, after subtracting contributions from the free ligand, was fitted to a one-site ligand binding model. Control experiments of free IAEDANS titrated with Lac or CR also showed ligand concentration-dependent quenching of the fluorophore. The apparent  $K_d$  values for these interactions are an order of magnitude higher than for the protein binding ( $19 \pm 2\ \mu\text{M}$  and  $154 \pm 6\ \mu\text{M}$  for CR and Lac respectively). Fitting the protein titration data to two independent binding events using the  $K_d$  derived from the control experiments were not successful indicating that specific binding of the compounds to the attached AEDANS is not likely to occur.

**Circular Dichroism Spectroscopy.** CD was measured on a Chirascan spectrometer (Applied photophysics) equipped with a Peltier temperature control system. The samples contained  $5\ \mu\text{M}$   $\alpha\text{S}$  in 25 mM Tris buffer pH 7.4, 100 mM NaCl with or without  $10\ \mu\text{M}$  to 0.5 mM of the compounds. Samples with the same compound concentrations but without any protein were used as references. The measurements were performed at  $10^{\circ}\text{C}$ ,  $25^{\circ}\text{C}$  and  $37^{\circ}\text{C}$  using a cell with 1 mm path length.

**Isothermal Titration Calorimetry.** ITC experiments were carried out using VP-ITC titration microcalorimeters (MicroCal) at  $25^{\circ}\text{C}$ .  $\alpha\text{S}$ , Lac and CR were dissolved in PBS buffer pH 7.4 and the samples were degassed before the measurements. Each experiment involved a preliminary  $2\ \mu\text{L}$  injection followed by 25–27 injections of  $10\ \mu\text{L}$  using a  $300\ \mu\text{L}$  syringe. The cell volumes were 1.416 or 1.4242 mL. ITC raw data was analyzed using Origin 7 (OriginLab Corporation). In the CR experiments  $2\ \mu\text{M}$   $\alpha\text{S}$  (in the cell) was titrated with 0.1 mM or 0.2 mM CR. In the Lac experiments,  $5\ \mu\text{M}$ , and  $100\ \mu\text{M}$   $\alpha\text{S}$  (in the cell) was titrated by 0.1 mM and 1 mM Lac respectively. For all the experiments, relevant reference experiments were performed by titrating the solution in the syringe into pure buffer.

**Dynamic Light Scattering.** DLS was measured using an ALV/CGS-3 compact goniometer system operating at 632.8 nm wavelength (ALV-GmbH). The samples were filtered through  $0.2\ \mu\text{m}$  filter before the measurements and the scattered light was detected at  $150^{\circ}$  angle. The samples contained 1 mM or 0.1 mM CR or 0.5–0.6 mM Lac in 25 mM Tris pH 7.4, 100 mM NaCl, and the data was recorded at  $25^{\circ}\text{C}$ . The acquired data was analyzed by the regularization algorithm in the ALV correlator 3.0 software (ALV-GmbH). Additional data for Lac was acquired using a Zetasizer Nano ZS instrument (Malvern Instruments) operating at 532 nm and a detection angle of  $173^{\circ}$ . The correlation data was exported and analyzed using the ALV software.

**Aggregation Assays.** Aggregation of  $\alpha\text{S}$  was assayed in  $100\ \mu\text{M}$  protein samples in 20 mM Tris buffer pH 7.4, 100 mM

NaCl with the addition of 0.01% NaN<sub>3</sub>, 500  $\mu$ L of protein sample were incubated at 37 °C under constant shaking at 300 rpm, and 50  $\mu$ L aliquots were withdrawn on a daily basis, assayed for thioflavine T (ThioT) binding (24, 34) and stored at 4 °C until the end of the assay for further determinations (SDS-PAGE and electron microscopy). Fibril formation was monitored by the ThioT assay (24, 34). Briefly, 10  $\mu$ L aliquots were diluted in 1 mL of 20  $\mu$ M ThioT and the fluorescence was measured in a FlashScan spectrofluorimeter (Jena Analytik), with an excitation wavelength of 446 nm. Emission wavelengths from 460 to 600 nm were collected and the integrated fluorescence between 470 and 490 nm was employed for determination of the relative content of  $\alpha$ S fibrils in the sample. Quenching of ThioT fluorescence by Lac and CR was assayed by incubating preformed fibrils for 30 min with various concentrations of compound (1  $\mu$ M to 1 mM), and measuring the ThioT fluorescence of the sample. The relative amount of insoluble protein was assayed by centrifuging the samples at 16000g and analyzing the supernatant fraction in 4–12% SDS-PAGE (Novex, Invitrogen). The amyloid-aggregated material was determined by resistance to solubilization with 1% Sarkosyl, by resolving the soluble fraction (nonamyloid) in a SDS-PAGE. Image quantization was performed on Coomassie-stained gels with the software ImageJ (NIH). Transmission electron microscopy (TEM) images at 25000 $\times$  magnification were obtained using a Phillips CEM100 transmission electron microscope (Imaging facility, Dept. of Pathology, University of Cambridge). 10  $\mu$ L of 1:10 dilution samples were applied on Formvar-coated nickel grids (Agar scientific) and stained with 2% (w/v) uranyl acetate.

## RESULTS

*Lac and CR Bind to Monomeric  $\alpha$ S.* The interaction of  $\alpha$ S with Lac and CR was initially investigated by heteronuclear NMR spectroscopy. Changes in chemical shifts and intensities of several peaks in the <sup>1</sup>H–<sup>15</sup>N correlation NMR spectrum of  $\alpha$ S, observed during titrations of the protein with increasing amounts of each compound, indicate that Lac and CR bind to the protein in a concentration dependent manner (Figure 1 and Figure S1 of the Supporting Information). The observed changes are more pronounced for CR than for Lac, which suggests different affinities for the ligands. The chemical shift perturbations report on changes in the chemical environment and/or in the relative populations of different conformations in the  $\alpha$ S structural ensemble. Both ligands affect the 100 most N-terminal residues of the protein significantly more than the C-terminus (Figure 1). Within this region, two broadly distinct binding domains can be identified with the first being approximately residues 1–40 and the second, residues 50–100. The latter domain includes the NAC region, which is believed to be the most aggregation-promoting segment of the protein (35, 36). The most N-terminal binding domain experiences a higher degree of peak intensity loss for both compounds while the region showing the largest chemical shift changes differs between the two binders; for CR, the largest shift changes are observed in the second binding domain (the region 50–77) although it cannot be excluded that even larger perturbations occur for residues in the N-terminal part that are too broad to be detected. Lac, on the other hand, mainly affects the chemical shifts of residues 1 to 22 in the N-terminal region.

*Ligand Binding Causes Exchange Broadening of  $\alpha$ S NMR Signals.* The changes in peak intensity observed in the <sup>1</sup>H–<sup>15</sup>N correlation spectrum of  $\alpha$ S bound to CR and Lac could

be due to several processes: (i) increase in the rotational and translational correlation times, e.g. by binding to large ligand aggregates or by ligand-induced oligomer formation of the protein itself; (ii) chemical exchange on the  $\mu$ s–ms time scale due to changes in the conformational properties of the  $\alpha$ S polypeptide ensemble and/or interaction with the ligands; (iii) changes in amide hydrogen exchange rates.

Alterations in peak intensities resulting from hydrogen exchange can be expected to result from interactions that alter the exposure of the peptide backbone to solvent. In order to exclude this effect as a cause for the changes in peak intensity, <sup>13</sup>C direct detected NMR experiments were performed on <sup>13</sup>C–<sup>15</sup>N-labeled  $\alpha$ S with and without CR and Lac (31). <sup>13</sup>CO–<sup>15</sup>N correlation spectra showed the same profiles for intensity changes as the <sup>1</sup>H–<sup>15</sup>N correlation (Figure 2a,b and Figure S2 of the Supporting Information) suggesting that hydrogen exchange effects are not a major cause of line broadening under these conditions. Furthermore (as described in detail below), PFG NMR experiments suggest that the line broadening observed upon ligand binding is not due to significant increases in the molecular size of the complexes, and points toward exchange broadening on a slow to intermediate time scale as the major cause for the decreased NMR peak intensity.

In order to probe whether complex formation perturbs the content of secondary structure in the ensemble of  $\alpha$ S conformations, we employed CD spectroscopy. The far-UV CD spectrum of  $\alpha$ S at 10 °C is in agreement with a largely unstructured protein (Figure 2c,d) as previously reported for  $\alpha$ S (7, 21, 37). The addition of increasing amounts of CR results in ellipticity changes at 196 and 220 nm (Figure 2c), similar to those reported for other structure-promoting conditions (21, 38, 39). Addition of Lac causes changes in the 196–200 nm region of the CD spectrum, similar to those seen with CR but with lower magnitude (Figure 2d). Similar, but less significant, changes in the  $\alpha$ S CD spectrum are observed for both compounds at higher temperatures (Figure S3 of the Supporting Information). Taken together, the NMR and CD data suggest that the ensemble of conformations populated by  $\alpha$ S is strongly perturbed upon binding to CR but is less affected by Lac.

*Lac and CR Form Supramolecular Assemblies in Solution.* The ability of CR itself to form aggregates or micelle-like species in solution is well-known (11–14), and self-assembly has as well been reported for some phenothiazines similar to Lac (40). The propensities of the compounds to self-associate were therefore investigated using DLS.

In 1 mM solution, the DLS data show that CR forms two types of species (Figure 3a). The smaller of these (representing the major population) has an  $R_H$  distribution centered around 1.9 nm, which is in agreement with other reports of CR self-assembly (11). Due to the elongated shape of the CR molecule this apparent  $R_H$  could correspond to the monomeric compound as well as a small oligomer. The larger particles have an  $R_H$  of approximately 40 nm (Figure 3a). At lower CR concentrations (0.1 mM), a similar size distribution is observed but with a slightly shifted average ( $\sim$ 1.4 nm) of the smaller species (Figure 3a). Such concentration dependence strongly suggests an oligomeric nature of this molecular species.

The use of DLS to investigate Lac self-assembly is limited by the overlap of its absorbance spectrum with the laser wavelengths of the DLS instruments. However, measurements from two instruments, operating at different wavelengths, indicate that Lac, at 0.5 mM concentration, does indeed form supramolecular

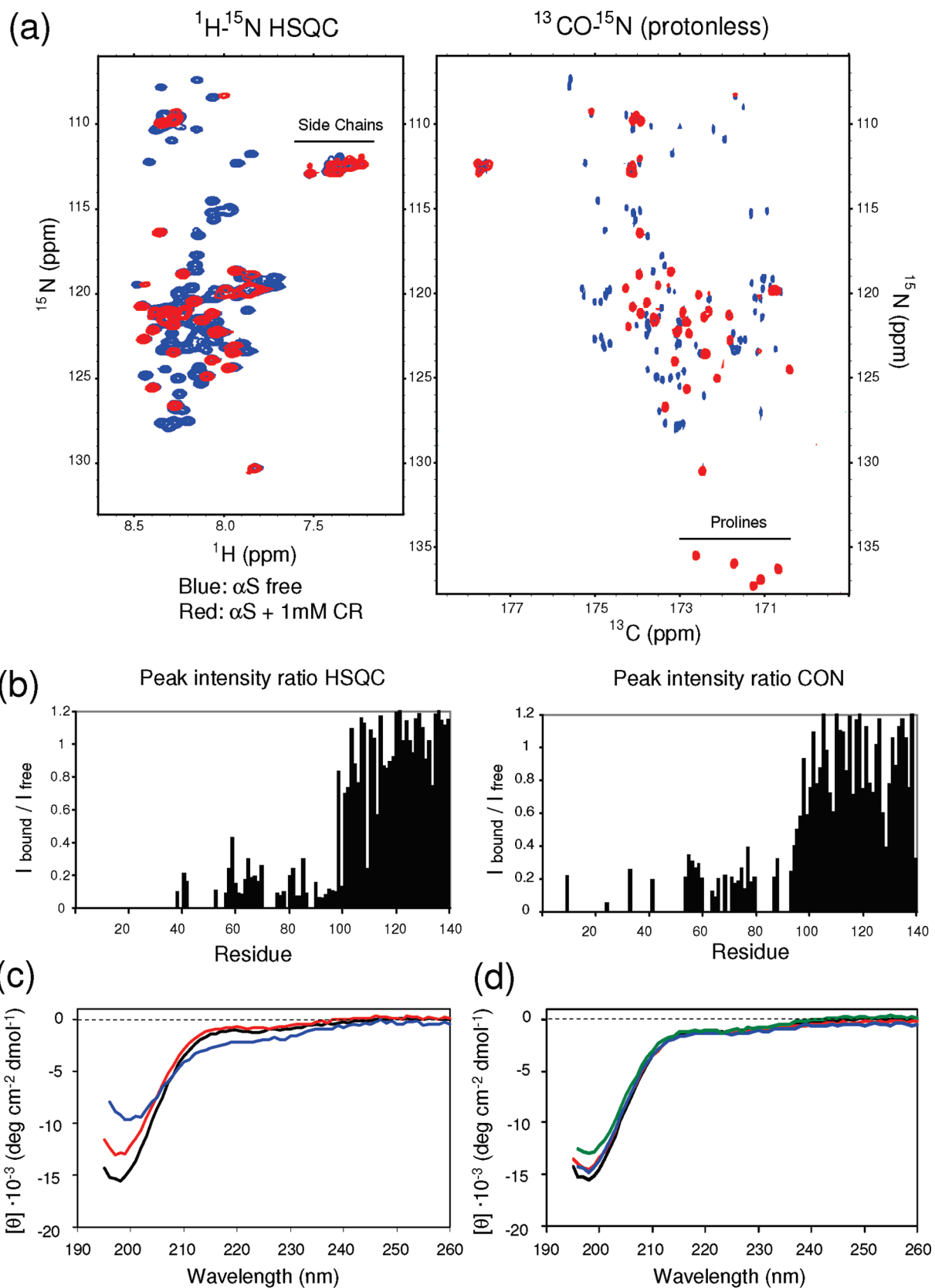


FIGURE 2: The compounds cause slow to intermediate conformational exchange in  $\alpha$ S. (a) Comparison of  $^1\text{H}$ - $^{15}\text{N}$  HSQC (left) and  $^{13}\text{C}$  direct detected  $^{13}\text{C}$ - $^{15}\text{N}$  correlation spectra (right) of 100  $\mu\text{M}$   $\alpha$ S with (red) and without (blue) 9:1 molar excess of CR. (b) Peak intensity ratios between bound and free protein are plotted below each spectrum. (c) Far-UV CD spectrum of 5  $\mu\text{M}$   $\alpha$ S at 10  $^\circ\text{C}$  free (black), with 10  $\mu\text{M}$  CR (red) and 0.1 mM CR (blue). (d) Far-UV CD spectrum of 5  $\mu\text{M}$   $\alpha$ S at 10  $^\circ\text{C}$  free (black), with 5  $\mu\text{M}$  Lac (red), with 50  $\mu\text{M}$  Lac (blue), and with 0.5 mM Lac (green).

aggregates. The average  $R_{\text{H}}$  of these species are approximately 15 and 90 nm for the two populations respectively (Figure 3b).

Opposite to CR, the larger assemblies represent the major population. The DLS data recorded for 0.1 mM Lac were

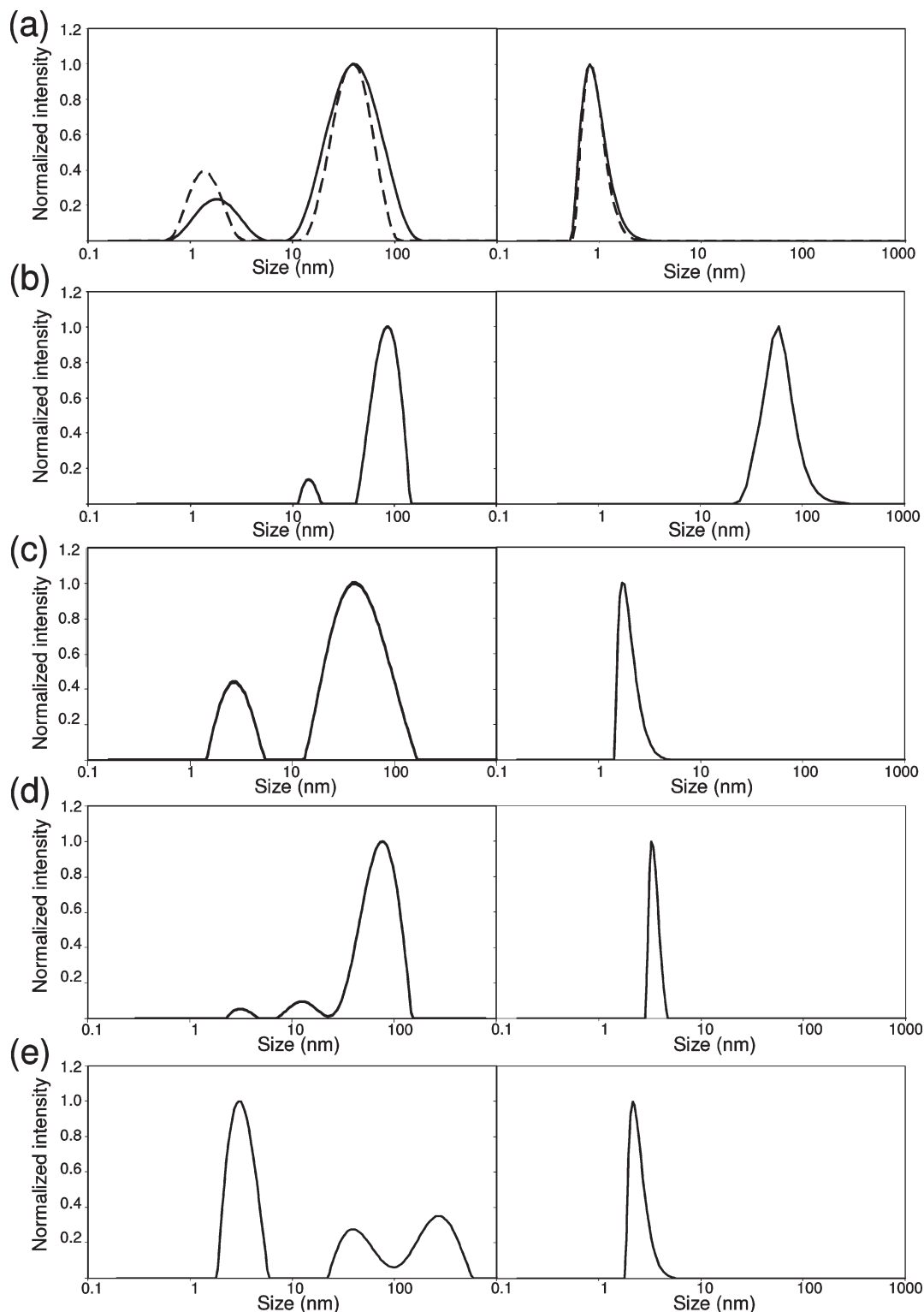


FIGURE 3: CR and Lac form supramolecular aggregates in solution. DLS derived size distributions of CR and Lac at 25 °C. The left panels show the normalized unweighted scattering intensity data and right panels the same data weighted by the number of molecules. The presented data represents averages of several measurements. (a) Size distribution of 1 mM (continuous line) and 0.1 mM (broken line) CR measured on the ALV instrument at 632.8 nm. (b) Representative size distribution of 0.5 mM Lac measured on the Zetasizer Nano instrument at 532 nm. (c) Size distribution of a sample containing 0.9 mM CR and 40  $\mu$ M  $\alpha$ S. (d) Size distribution of a sample containing 0.6 mM Lac and 50  $\mu$ M  $\alpha$ S. (e) Size distribution of a sample with 50  $\mu$ M  $\alpha$ S shown as reference.

inconclusive (data not shown), most likely because of sample absorbance, and neither confirms nor excludes the presence of aggregated species.

The tendency of Lac to self-associate was further investigated by NMR spectroscopy. The intensities/integrals of the Lac signals in the 1D NMR spectrum at 0.5 mM total Lac

concentration were found to be significantly lower than what would be expected for a monomeric compound of low molecular weight (Figure S4 of the Supporting Information), which, in line with the DLS data, strongly suggests the presence of a substantial population of large species. Using the high intensity Tris buffer peak (25 mM peak at 3.7 ppm) as an integration reference, the

concentrations of the visible (small) Lac species were found to be approximately 20  $\mu\text{M}$ , representing 4% of the total Lac present. PFG NMR experiments indicate that these species have similar diffusion properties as the Tris buffer (data not shown) suggesting that the observed peaks most likely arise from monomeric Lac.

*The Interaction with  $\alpha\text{S}$  Is Mediated by Monomeric and/or Small Oligomeric Compound Species.* PFG NMR experiments were used to monitor the diffusion properties, and thereby the molecular dimensions, of  $\alpha\text{S}$  in the absence and presence of the two ligands. The effective  $R_H$  of free  $\alpha\text{S}$  was found to be  $29.2 \pm 0.2 \text{ \AA}$  (Figure 4a,b and Figure S5 of the Supporting Information), which is in good agreement with previous reports (41, 42). This number is also in agreement with DLS measurements of free  $\alpha\text{S}$  (Figure 3e). Addition of CR induced a more compact conformational ensemble (effective  $R_H = 25.0 \pm 0.3 \text{ \AA}$ ) while the  $R_H$  for  $\alpha\text{S}$  in the presence of Lac is only slightly larger than without the compound ( $30.6 \pm 0.3 \text{ \AA}$ ). These data suggest that the formed complexes are of similar size as the free protein and binding species correspond to monomers or small oligomers of the compound. These observations are confirmed by DLS experiments of  $\alpha\text{S}$  in presence of the compounds. In samples containing 40–50  $\mu\text{M}$   $\alpha\text{S}$  and 0.9 mM CR, the protein peak at  $R_H = 2.8 \text{ nm}$  was indeed the major population (Figure 3c). In the presence of 0.6 mM Lac, similarly, the major population detected corresponded to monomeric  $\alpha\text{S}$  binding to a small oligomer of Lac  $R_H = 3.3 \text{ nm}$ . Notably, complex formation appears to strongly shift the size distribution of Lac species.

To explore further a potential 1:1 binding of CR to  $\alpha\text{S}$ , additional NMR experiments were carried out at low micromolar concentrations. The  $^1\text{H}$ – $^{15}\text{N}$  correlation spectrum of 1  $\mu\text{M}$   $\alpha\text{S}$  with 4  $\mu\text{M}$  CR shows substantial line broadening of the 100 most N-terminal residues, most of them beyond detection (Figure 4c). This result is closely similar to the observations of the high concentration experiments (see above) and suggests that CR interacts with monomeric  $\alpha\text{S}$  at a low  $\mu\text{M}$  concentration which is below its reported critical concentration for self-association (13).

*Affinities and Thermodynamics of the  $\alpha\text{S}$ :Ligand Interactions.* The thermodynamic characteristics of the binding events of CR and Lac to  $\alpha\text{S}$  were investigated using ITC. Control titration of CR into buffer shows substantially larger endothermic heats for the first few injections compared to later ones (Figure 5a), suggesting that CR is in an aggregated state in the syringe. Such calorimetric behavior is typically observed for disaggregation of micellar surfactants (43, 44) and has previously been reported for CR (45). Similar results were observed for 1.0 mM Lac titrated into buffer (Figure 5b), which confirms the presence of oligomeric species observed by DLS. Titration of 0.1 mM Lac into buffer, however, showed exothermic heat effects as expected for a process dominated by the heat of dilution (Figure 5b). The self-association properties of Lac thus seem to change precisely in this concentration interval.

Titrations of 0.2 mM (Figure 5a) and 0.1 mM (data not shown) CR into 2  $\mu\text{M}$   $\alpha\text{S}$  solution indicated a one-site interaction mechanism where several ligand molecules ( $\sim 8$ ) of CR bind to the protein with a  $K_d$  of 0.4–1  $\mu\text{M}$ . This could reflect the binding of small oligomeric CR species or several individual CR molecules binding with similar affinities in a cooperative process. The binding process is entropically driven with a small favorable enthalpy contribution, which is in agreement with CR binding to hydrophobic patches of  $\alpha\text{S}$ .

ITC experiments with the Lac: $\alpha\text{S}$  system confirm the lower affinity of this compound compared to CR. Titration of 0.1 mM

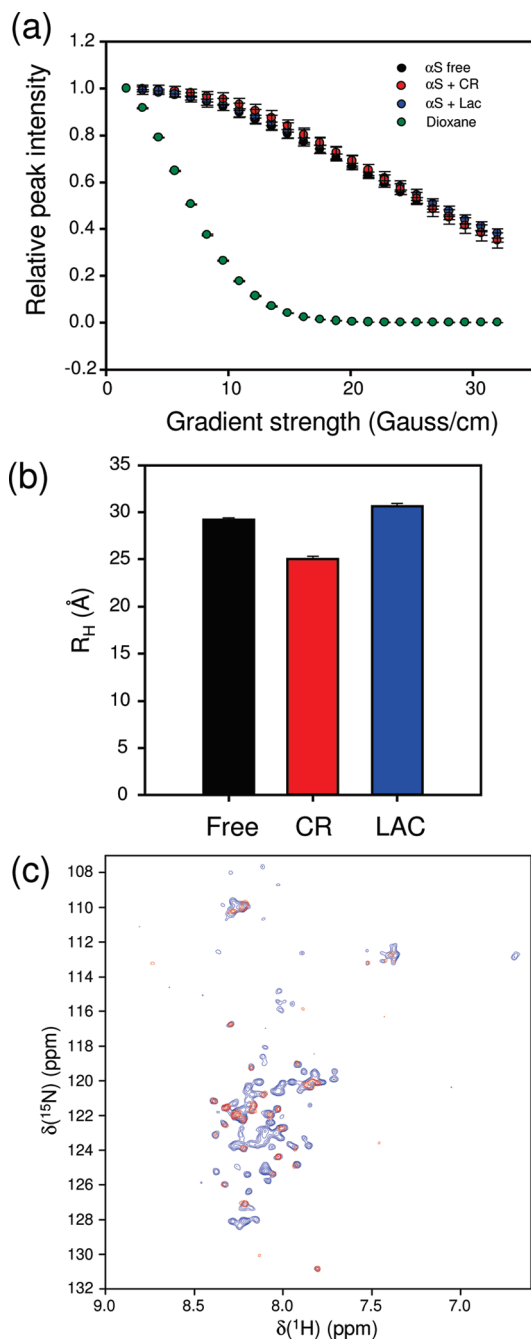


FIGURE 4: The compounds bind to  $\alpha\text{S}$  as small oligomeric aggregates. (a) PFG NMR data measured for  $\alpha\text{S}$  in the absence and presence of CR and Lac. The peak intensities (integrals) as function of the employed gradient strengths for dioxane and 100  $\mu\text{M}$   $\alpha\text{S}$  in the absence and presence of 9 mol equiv CR or 6 mol equiv of Lac. (b) Data from PFG NMR were fitted to single Gaussian functions, and the rates of decay were converted into hydrodynamic radii. (c)  $^1\text{H}$ – $^{15}\text{N}$  SOFAST-HMQC spectrum of 1  $\mu\text{M}$   $\alpha\text{S}$  in the absence (blue) and presence (red) of 4  $\mu\text{M}$  CR.

Lac into 5  $\mu\text{M}$   $\alpha\text{S}$  does not result in significant heat changes (data not shown); however, small exothermic heat effects were generated when 1.0 mM Lac was titrated into 100  $\mu\text{M}$   $\alpha\text{S}$  (Figure 5b). The small magnitude of the measured heat output offers an explanation for why no interaction was detected in the low concentration experiments and suggests an entropically driven binding process, as observed for CR. The absence of signal baseline recovery at the end of the titration indicates that the binding process does not reach saturation and prohibits the

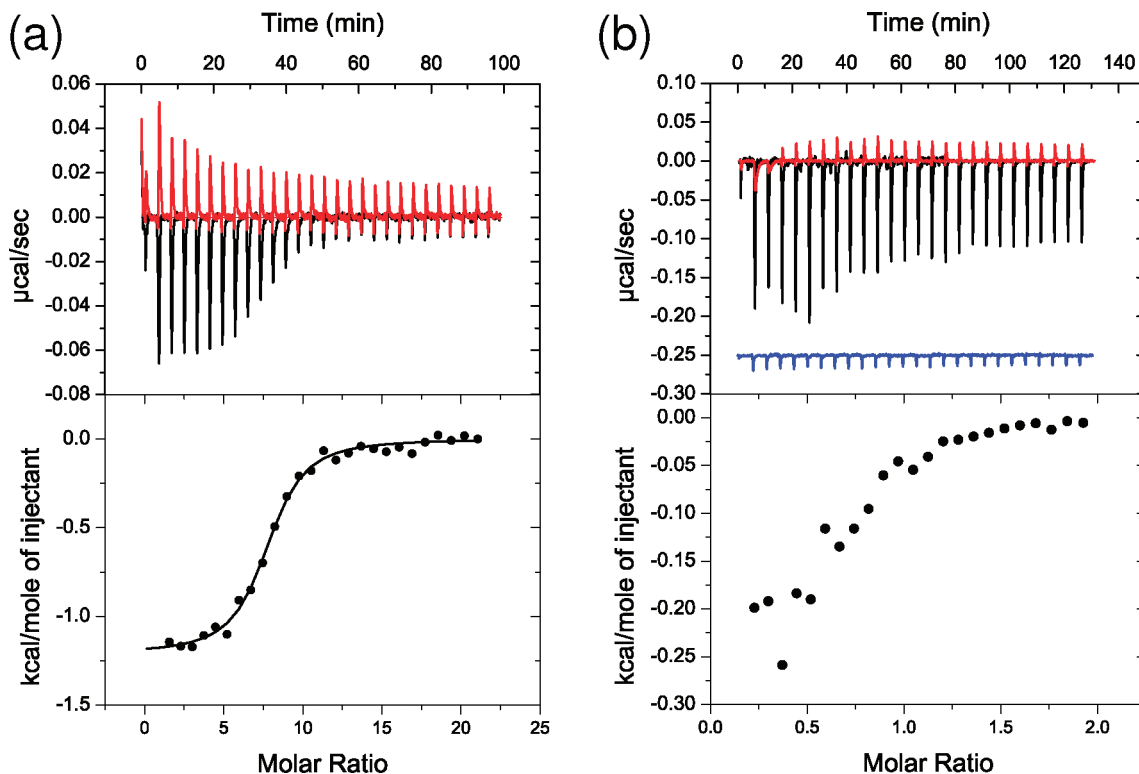


FIGURE 5: Calorimetric characterization of the interactions between the small molecules and  $\alpha$ S. Baseline corrected ITC raw data (top) and integrated heat data (bottom) of CR and Lac titrated into  $\alpha$ S solution and pure PBS buffer at 25 °C. (a) 0.2 mM CR titrated into buffer (red) and 2  $\mu$ M  $\alpha$ S (black). The best fit of the integrated data to a one-site model is shown as a black line and corresponds to 8 CR molecules binding with a  $K_d = 0.4 \mu$ M. (b) 1 mM Lac titrated into buffer (red) or 100  $\mu$ M  $\alpha$ S (black). The baseline corrected raw data of 0.1 mM Lac titrated into buffer is also included (blue line at  $-0.25 \mu$ cal/sec for better comparison) to show the concentration dependence of the heat of dilution.

determination of any dissociation constant or binding stoichiometry.

The relative affinities of the  $\alpha$ S:ligand complexes were then estimated from the quenching of the fluorescence emission of AEDANS-conjugated  $\alpha$ S upon titration with the compounds. The fluorophore was specifically attached to a cysteine residue introduced by mutagenesis in the vicinity of the NMR-derived binding regions (position 24 for Lac and 62 for CR). Fluorescently labeled proteins were titrated with the compounds and a dose-dependent reduction of fluorescence intensity was observed (Figure 6). Fitting the data to a single site binding model resulted in apparent  $K_d$  of  $1.05 \pm 0.05 \mu$ M for CR and  $12 \pm 2 \mu$ M for Lac. These data thus confirm the ITC derived affinity for CR and also provide an apparent  $K_d$  for Lac. The observed lower binding affinity of Lac compared to CR is in good agreement with NMR experiments described above.

**Specificity of CR and Lac Interactions with  $\alpha$ S.** In order to evaluate the specificity of the compounds for  $\alpha$ S, we studied the binding behavior of  $\beta$ -synuclein ( $\beta$ S), a closely related protein which does not aggregate under pathological conditions.  $\beta$ S also lacks a defined secondary structure in solution and populates a highly dynamic ensemble of conformations (42), however it does not readily fibrillate due to the absence of a stretch of highly hydrophobic amino acids in the central region of the protein (46). Employing  $^1\text{H}$ - $^{15}\text{N}$  correlation NMR experiments we found that  $\beta$ S is able to bind both CR and Lac in a similar fashion to  $\alpha$ S (Figure S6 of the Supporting Information), suggesting that the compounds do not discriminate between amyloidogenic and nonamyloidogenic conformers.

As an additional control for the specificity of the binding mechanisms of the compounds, the heteronuclear NMR experiments

were repeated in presence of bovine serum albumin (BSA). This test is commonly used for determining the promiscuity of binding by small molecule ligand (14, 15). Addition of 25 mg/mL (8:1 BSA: $\alpha$ S molar ratio) BSA to  $\alpha$ S samples containing CR or Lac resulted in a dramatic change of the NMR resonances (Figure S6 of the Supporting Information). The line broadening observed in the majority of the N-terminal peaks due to compound addition almost fully disappeared, and peaks along the whole sequence became visible again. This clearly shows that BSA competes with  $\alpha$ S for the binding of both compounds in a similar way as has been reported for promiscuous inhibitors (14, 15). The results also show that the binding of the compounds to  $\alpha$ S are reversible events.

**CR and Lac Modulate Differently the  $\alpha$ S Aggregation Pathway.** The effect of CR and Lac on  $\alpha$ S aggregation and fibril formation was investigated by incubating the protein with various concentrations of the ligands. Both compounds have previously been reported to inhibit the formation of amyloid fibrils by  $\alpha$ S (3), and, as determined by reduced ThioT fluorescence, they seem to affect the  $\alpha$ S fibril formation significantly, even at very low stoichiometric ratios (Figure 7a,b). Interestingly, however, protein aggregates were visible in most of the incubated samples. This observation could be due to the presence of nonamyloid aggregates that do not bind ThioT or to specific reduction of ThioT fluorescence by the compounds as a result of quenching or competition of binding sites in the fibrillar species. The potential influence on ThioT fluorescence by the compounds was investigated by adding dye to mature compound-free  $\alpha$ S fibrils, preincubated with Lac or CR, and comparing the observed fluorescence with a negative (compound-free) control. The results clearly show that high concentrations of

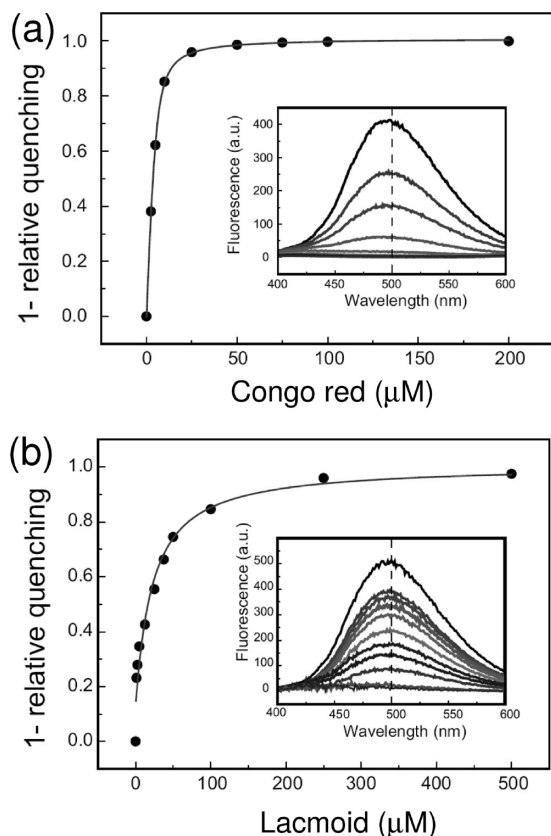


FIGURE 6: Relative affinities of  $\alpha$ S:ligand interactions. Fluorescence quenching experiments, using  $5 \mu\text{M}$  AEDANS-conjugated  $\alpha$ S, show that CR (a) binds  $\alpha$ S more strongly than Lac (b). Quenching data fitted to a single-site binding model yields apparent  $K_d$  values of  $1.05 \pm 0.05 \mu\text{M}$  for CR (a) and  $12 \pm 2 \mu\text{M}$  for Lac (b). The fluorescence raw data in the absence (top line) and presence of  $2.5 \mu\text{M}$  to  $0.2 \text{ mM}$  CR (a) and  $1 \mu\text{M}$  to  $0.5 \text{ mM}$  Lac (b) are shown as insets.

the compounds alter the ThioT fluorescence of the fibrils (Figure 7c,d). However, the influence on ThioT fluorescence of low concentrations of the compounds is not significant.

To verify further the presence of aggregated protein material, the amount of soluble protein in the samples was evaluated at different time points of the aggregation assays by centrifuging an aliquot at  $16000g$  and analyzing the protein remaining in the supernatant using SDS-PAGE. The results confirm the presence of insoluble protein aggregates in all the conditions studied (Figure 7e,f). Only in samples containing 5:1 molar excess of Lac does  $\alpha$ S remain in a monomeric soluble form until the end of the assay. Indeed, treatment of aggregated protein with 1% sarkosyl, a detergent capable of solubilizing amorphous aggregates but not mature amyloid fibrils, shows an increased amount of soluble protein both in control experiments and with the compounds. While Lac addition does not show differences with the control at concentrations of  $50 \mu\text{M}$  or lower, CR increases the extent of Sarkosyl soluble protein even at low concentrations (Figure 7e,f).

Such observations are corroborated by TEM of the aggregated samples at the end of the assays. In the control experiment (i.e., no added ligands)  $\alpha$ S formed fibrils as expected (Figure 7h) (21, 36). Incubation with low concentrations of Lac does not, under the applied experimental conditions, distinctively change the morphology of the fibrillar material (Figure 7h). However, incubation with  $10 \mu\text{M}$  CR produces amorphous aggregates as well as fibrillar species (Figure 7g). At higher CR

concentrations, some fibrils are visible but amorphous aggregates are still the dominating morphology (Figure 7g). Interestingly, in the samples incubated with  $0.5 \text{ mM}$  Lac, no aggregates are visible (Figure 7h), confirming its ability to reduce the overall protein insolubilization.

## DISCUSSION

A variety of compounds have been reported to interact with  $\alpha$ S and inhibit its aggregation and/or fibril formation (3, 6, 47–52). However, the molecular mechanisms for their action are, in most cases, only vaguely understood. We have conducted an extensive characterization of the protein:ligand interactions at a residue-specific resolution, together with a careful description of the effects on  $\alpha$ S aggregation, in an attempt to provide a picture of the inhibition mechanisms for CR and Lac.

The heteronuclear NMR data show that CR and Lac mainly interact with the N-terminal and central regions of  $\alpha$ S. Of the two compounds, CR binds more strongly and has a more pronounced affinity for the aggregation-prone NAC region, features that might be related to the presence of negative charges (7). Moreover, CR and Lac interactions differently perturb the ensemble of structures populated by  $\alpha$ S, as shown by NMR and CD data. In both cases NMR resonance intensities are lost due to line broadening, mainly caused by conformational exchange on a slow-intermediate time scale. For CR, the observed changes in secondary structure content are accompanied by a reduction in the hydrodynamic radius of the  $\alpha$ S complex, while Lac has less effect on the secondary structure content and the hydrodynamic radius. These observations could, in principle, be interpreted in terms of the accumulation of specific intermediate states, as previously suggested for other effectors of  $\alpha$ S aggregation (21), but it is more likely that they represent changes in the population distribution across the conformational energy landscape of the protein.

The self-association characteristic of the compounds indeed complicates the analysis of the binding mechanisms. Based on the diffusion measurements, interactions between monomeric  $\alpha$ S and large colloidal species can be excluded, which leaves the options that the interaction is mediated by monomeric or small oligomeric compound species. Our findings point to small oligomeric compound species as the main effectors; however, weak 1:1 interactions cannot be excluded. The presence of small oligomeric CR species is supported by DLS, and the ITC data imply a mechanism where several CR molecules bind to each  $\alpha$ S molecule. The apparent 1:1 binding between the compounds and  $\alpha$ S observed with fluorescence quenching experiments could actually be a 1: $n$  binding if the compounds bind as an oligomer to a single site on the protein. Previous studies reported the binding of several CR molecules to different types of proteins (11, 53, 54) indicating that multivalent binding is characteristic of CR regardless of the nature of the specific protein involved. The critical concentration of CR needed to form aggregates has been reported to be approximately  $5 \mu\text{M}$  (13), suggesting that the binding observed by NMR at low micromolar CR concentrations might represent a 1:1 interaction. However, the self-association ability is most likely modulated by factors such as pH, ionic strength and temperature which could lower the critical concentration for CR to form soluble aggregates. In addition, the presence of  $\alpha$ S itself could affect this concentration, as shown for certain aggregation promoting detergents (55).

In the case of Lac, the absence of binding site saturation in the ITC prevents the determination of the stoichiometry. Such behavior could indicate a mechanism of binding involving several

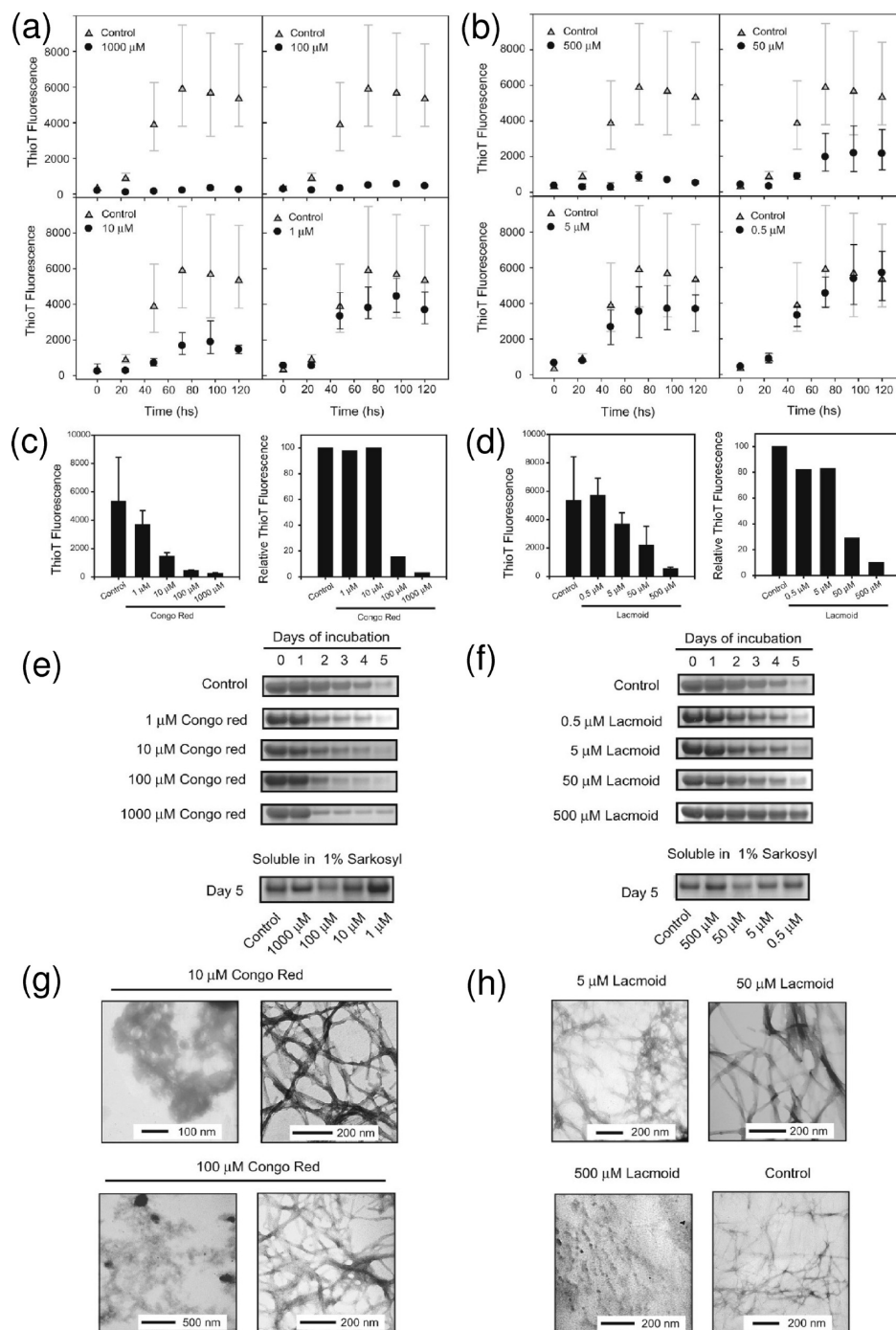


FIGURE 7: CR and Lac exhibit different mechanisms of inhibition of  $\alpha$ S amyloid formation. (a, b) Aggregation assays were performed on  $100 \mu\text{M}$   $\alpha$ S in the presence of  $0.5 \mu\text{M}$  to  $1 \text{ mM}$  of the compounds. ThioT fluorescence traces as function of time in absence (control) and presence of varying amounts of CR (a) and Lac (b). (c, d) The compounds cause interference of the ThioT signal in a concentration dependent manner. ThioT fluorescence of the samples after 5 days of incubation in absence (control) and presence of varying amounts of CR (c, left plot) and Lac (d, left plot). ThioT fluorescence interference (quenching or competition) determined by incubating preformed amyloid fibrils for 30 min with CR (c, right plot) and Lac (d, right plot). The results are expressed as relative to the fluorescence of the control (incubation with buffer). (e, f) SDS-PAGE of protein remaining soluble along the aggregation assays in the absence (control) and presence of various concentrations of CR (e, top panel) and Lac (f, top panel). Sarkosyl solubilization of pellets from the final point of the aggregation assay in the presence of CR (e, bottom panel) and Lac (f, bottom panel). (g, h) TEM images of the aggregates corresponding to the end products from the aggregation assays without (control) and with CR or Lac.

Lac molecules per  $\alpha$ S molecule or a competition between ligand: ligand and ligand:protein interactions, reducing the effective concentration of binding competent species for the latter. The reference ITC experiments indicate a change of the self-association properties of Lac in the range  $0.1\text{--}0.5 \text{ mM}$ , and the critical aggregation concentrations have indeed been reported to be in the  $\text{mM}$  range for other phenothiazine compounds (40). Hence,

besides the intrinsic chemical properties of the compounds, the observed difference in binding affinity could be related to the difference in critical concentrations of aggregation as well as the propensities to form oligomeric species of appropriate size and structure.

The apparent  $K_d$  values for the CR and Lac complexes with  $\alpha$ S are in the low micromolar region, which represent binding of

moderate strength. Such interactions are expected to be easily competed out, which indeed is observed by addition of BSA. Albumin is well-known to bind a variety of different small molecules, such as negatively charged compounds (56), and has been shown to interact with small oligomers of CR (53). Our results strongly suggest that BSA interacts with both CR and Lac by binding to either or both monomeric and small oligomeric species. Previous studies of CR binding to globular proteins, such as immunoglobulin light chain variable domain (45) and human growth hormone (9), have also reported  $K_d$  values in the micromolar range.

The differences in the interaction mechanisms for the two compounds are also reflected in their anti-amyloid behavior. For CR we observe an increased proportion of amorphous aggregates at very low concentrations, accompanied with a more rapid loss of soluble material compared to the reference experiment (Figure 7). On the basis of these observations, we hypothesize that binding of CR to  $\alpha$ S induces conformational changes that weaken the (protective) interactions of the native state allowing the formation of new intermolecular interactions between the N-terminal and C-terminal part of the protein. These events direct the protein into an alternative pathway leading to amorphous aggregates that might be kinetically more favorable compared to fibrils. The interaction with the NAC region might also impair with the formation of amyloid-like structures. Moreover, the fact that CR has high affinity for amyloid fibrils could render early amyloid nuclei incompatible for elongation, stabilizing oligomers and amorphous aggregates. Lac, on the other hand, seems to stabilize a native-like state with the concomitant protection of the NAC region of  $\alpha$ S and thereby inhibit self-assembly. The effect is, however, only observed at high concentrations of the compound, which could be related to the lower self-association ability compared to CR. Another source for the different inhibitory effects could be the charge differences between the compounds. Negatively charged surfaces have been suggested to promote protein aggregation (57), and anionic detergents have indeed been shown to accelerate  $\alpha$ S self-association while uncharged detergent did not have this effect (55). The effect on  $\alpha$ S aggregation observed for CR might thus be a rather complex process resulting from a combination of aggregation promoting and inhibitory effects.

Interestingly, CR and Lac also differ in the mechanisms by which they inhibit aggregation of the  $A\beta$  peptide (4). In agreement with our results, Lac inhibits the formation of all types of  $A\beta$  aggregates. CR, on the other hand, appeared to inhibit formation of oligomers but not fibrils. During the preparation of this manuscript, Rao and co-workers (7) presented an NMR and CD study of the CR and Lac interactions with  $\alpha$ S. Our results agree well with theirs regarding that the compounds interact with monomeric  $\alpha$ S and the observed binding sites on  $\alpha$ S. However, a broad multidisciplinary experimental strategy allows us to characterize the differences between the compounds with respect to the binding mechanisms, affinities and effects on amyloid formation. Furthermore, our detailed investigation establishes the critical role of the self-association of the small molecules for their interaction with  $\alpha$ S.

Recently it was suggested that self-association might be a common property among aggregation inhibitors and that the inhibition would be a result of sequestering the protein molecules to large colloidal particles (15). Our data confirm that both CR and Lac are able to self-associate into such particles. However, the binding of the compounds to monomeric  $\alpha$ S proceeds via

interactions with small oligomeric species. Such species could be pre-existing or formed as a consequence of binding to the protein. In both cases, the self-association abilities of the compounds are of critical importance. This type of compounds, especially CR, has been reported to interact with a wide range of proteins, which is indeed confirmed by the observed BSA competition. However, their mechanisms of action might be of particular importance when binding to intrinsically unstructured proteins because of their ability to provide a large interaction surface that could compensate for the entropic cost of binding. This might be an explanation for their frequent occurrence as aggregation inhibitors. The full impact of these findings remains to be investigated, but it is indeed notable that self-associating small molecules have shown anti-amyloid effects *in vivo* (8, 15, 58, 59), and it has been suggested that the self-association properties could also be of relevance for oral drug delivery (60).

## CONCLUSIONS

Our investigation illustrates well the complexity associated with the discovery and *in vitro* characterization of aggregation inhibition mechanisms of small molecules. We show that a broad biophysical approach is needed to obtain a complete characterization of such systems and to avoid false conclusions based on experimental artifacts such as low specificity or quenching of ThioT fluorescence by the tested compounds. This approach allows us to describe the mechanisms by which CR and Lac affect the amyloid fibril formation of  $\alpha$ S. Our experiments show that CR and Lac bind to monomeric  $\alpha$ S as small oligomeric species, although to alternate regions and with different affinities, and that these binding events are directly responsible for affecting the fibril formation of  $\alpha$ S in distinct ways. These differences can be attributed to the chemical nature of the compounds as well as their abilities to self-associate. Our results differ from reported cases in which such compounds inhibit the biochemical function of enzymes and the aggregation of other misfolding proteins in a promiscuous fashion by forming macroassemblies (14). These findings provide potential explanations for the nonspecific anti-amyloid effect observed for these compounds as well as important mechanistical information for future drug discovery efforts targeting the misfolding and aggregation of intrinsically unstructured proteins.

## ACKNOWLEDGMENT

We thank Prof. Astrid Gräslund (Stockholm University) for the use of DLS, CD, and NMR equipment; Dr. Verna Frasca (MicroCal), Louise Creagh (University of British Columbia) and Dr. Terence Hui (Elan Pharmaceuticals) for their assistance with the ITC experiments; Dr. Don Walker (Elan Pharmaceuticals) for LC/MS analyzes; Dr. Shang-Te D. Hsu (University of Cambridge) for the setup of  $^{13}\text{C}$  detected NMR experiments; Dr. Rick Arthis (Elan Pharmaceuticals) for critical review of the manuscript and for his suggestions; and the staff of the Biomolecular NMR facility at the Department of Chemistry, University of Cambridge.

## SUPPORTING INFORMATION AVAILABLE

Comparison of  $^1\text{H}$ - $^{15}\text{N}$  correlation NMR spectra of  $\alpha$ S in presence and absence of the investigated compounds (Figure S1), comparison of  $^{13}\text{C}$ - $^{15}\text{N}$  correlation NMR spectra of  $\alpha$ S in presence and absence of Lac (Figure S2), CD spectra of  $\alpha$ S in

presence and absence of the investigated compounds at three different temperatures (Figure S3), 1D NMR spectrum of Lac (Figure S4), detailed analysis of pulsed field gradient NMR data measured for  $\alpha$ S (Figure S5), and binding of the compounds to  $\beta$ S and the effect of BSA on the binding of the compounds to  $\alpha$ S investigated using  $^1\text{H}$ - $^{15}\text{N}$  correlation NMR (Figure S6). This material is available free of charge via the Internet at <http://pubs.acs.org>.

## REFERENCES

- Chiti, F., and Dobson, C. M. (2006) Protein misfolding, functional amyloid, and human disease. *Annu. Rev. Biochem.* 75, 333–366.
- Uversky, V. N., and Fink, A. L. (2004) Conformational constraints for amyloid fibrillation: the importance of being unfolded. *Biochim. Biophys. Acta* 1698, 131–153.
- Masuda, M., Suzuki, N., Taniguchi, S., Oikawa, T., Nonaka, T., Iwatsubo, T., Hisanaga, S., Goedert, M., and Hasegawa, M. (2006) Small molecule inhibitors of  $\alpha$ -synuclein filament assembly. *Biochemistry* 45, 6085–6094.
- Necula, M., Kaye, R., Milton, S., and Glabe, C. G. (2007) Small molecule inhibitors of aggregation indicate that amyloid  $\beta$  oligomerization and fibrillation pathways are independent and distinct. *J. Biol. Chem.* 282, 10311–10324.
- Cookson, M. R. (2006) Hero versus antihero: the multiple roles of  $\alpha$ -synuclein in neurodegeneration. *Exp. Neurol.* 199, 238–242.
- Ehrnhoefer, D. E., Bieschke, J., Boeddrich, A., Herbst, M., Masino, L., Lurz, R., Engemann, S., Pastore, A., and Wanker, E. E. (2008) EGCG redirects amyloidogenic polypeptides into unstructured, off-pathway oligomers. *Nat. Struct. Mol. Biol.* 15, 558–566.
- Rao, J. N., Dua, V., and Ulmer, T. S. (2008) Characterization of  $\alpha$ -synuclein interactions with selected aggregation-inhibiting small molecules. *Biochemistry* 47, 4651–4656.
- Frid, P., Anisimov, S. V., and Popovic, N. (2007) Congo red and protein aggregation in neurodegenerative diseases. *Brain Res. Rev.* 53, 135–160.
- Sereikaite, J., and Bumelis, V. (2006) Congo red interaction with  $\alpha$ -proteins. *Acta Biochim. Pol.* 53, 87–92.
- Khurana, R., Uversky, V. N., Nielsen, L., and Fink, A. L. (2001) Is congo red an amyloid-specific dye? *J. Biol. Chem.* 276, 22715–22721.
- Stopa, B., Piekarska, B., Konieczny, L., Rybarska, J., Spólnik, P., Zemanek, G., Roterman, I., and Król, M. (2003) The structure and protein binding of amyloid-specific dye reagents. *Acta Biochim. Pol.* 50, 1213–1227.
- Iyer, S. R. S., and Singh, G. S. (1970) Studies on the aggregation of dyes in aqueous solutions. *Kolloid-Z. Z. Polym.* 242, 1196–1200.
- Edwards, R. A., and Woody, R. W. (1979) Spectroscopic studies of cibacron blue and congo red bound to dehydrogenases and kinases. Evaluation of dyes as probes of the dinucleotide fold. *Biochemistry* 18, 5197–5204.
- McGovern, S. L., Caselli, E., Grigorieff, N., and Shoichet, B. K. (2002) A common mechanism underlying promiscuous inhibitors from virtual and high-throughput screening. *J. Med. Chem.* 45, 1712–1722.
- Feng, B. Y., Toyama, B. H., Wille, H., Colby, D. W., Collins, S. R., May, B. C. H., Prusiner, S. B., Weissman, J., and Shoichet, B. K. (2008) Small-molecule aggregates inhibit amyloid polymerization. *Nat. Chem. Biol.* 4, 197–199.
- Uversky, V. N. (2007) Neuropathology, biochemistry, and biophysics of  $\alpha$ -synuclein aggregation. *J. Neurochem.* 103, 17–37.
- Spillantini, M. G., Schmidt, M. L., Lee, V. M., Trojanowski, J. Q., Jakes, R., and Goedert, M. (1997)  $\alpha$ -synuclein in lewy bodies. *Nature* 388, 839–840.
- Eliez, D., Kutluay, E., Bussell, R. J., and Browne, G. (2001) Conformational properties of  $\alpha$ -synuclein in its free and lipid-associated states. *J. Mol. Biol.* 307, 1061–1073.
- Dedmon, M. M., Lindorff-Larsen, K., Christodoulou, J., Vendruscolo, M., and Dobson, C. M. (2005) Mapping long-range interactions in  $\alpha$ -synuclein using spin-label NMR and ensemble molecular dynamics simulations. *J. Am. Chem. Soc.* 127, 476–477.
- Bertoncini, C. W., Jung, Y., Fernandez, C. O., Hoyer, W., Griesinger, C., Jovin, T. M., and Zweckstetter, M. (2005) Release of long-range tertiary interactions potentiates aggregation of natively unstructured  $\alpha$ -synuclein. *Proc. Natl. Acad. Sci. U.S.A.* 102, 1430–1435.
- Uversky, V. N., Li, J., and Fink, A. L. (2001) Evidence for a partially folded intermediate in  $\alpha$ -synuclein fibril formation. *J. Biol. Chem.* 276, 10737–10744.
- Ulmer, T. S., Bax, A., Cole, N. B., and Nussbaum, R. L. (2005) Structure and dynamics of micelle-bound human  $\alpha$ -synuclein. *J. Biol. Chem.* 280, 9595–9603.
- Bodner, C. R., Dobson, C. M., and Bax, A. (2009) Multiple tight phospholipid-binding modes of  $\alpha$ -synuclein revealed by solution NMR spectroscopy. *J. Mol. Biol.* 390, 775–790.
- Hoyer, W., Antony, T., Cherny, D., Heim, G., Jovin, T. M., and Subramaniam, V. (2002) Dependence of  $\alpha$ -synuclein aggregate morphology on solution conditions. *J. Mol. Biol.* 322, 383–393.
- Delaglio, F., Grzesiek, S., Vuister, G. W., Zhu, G., Pfeifer, J., and Bax, A. (1995) NMRPipe: a multidimensional spectral processing system based on Unix pipes. *J. Biomol. NMR* 6, 277–293.
- Vranken, W. F., Boucher, W., Stevens, T. J., Fogh, R. H., Pajon, A., Llinas, M., Ulrich, E. L., Markley, J. L., Ionides, J., and Laue, E. D. (2005) The CCPN data model for NMR spectroscopy: development of a software pipeline. *Proteins* 59, 687–696.
- Croke, R. L., Sallum, C. O., Watson, E., Watt, E. D., and Alexandrescu, A. T. (2008) Hydrogen exchange of monomeric  $\alpha$ -synuclein shows unfolded structure persists at physiological temperature and is independent of molecular crowding in *Escherichia coli*. *Protein Sci.* 17, 1434–1445.
- Schleucher, J., Schwendinger, M., Sattler, M., Schmidt, P., Schedletzky, O., Glaser, S. J., Sørensen, O. W., and Griesinger, C. (1994) A general enhancement scheme in heteronuclear multidimensional NMR employing pulsed field gradients. *J. Biomol. NMR* 4, 301–306.
- Dedmon, M. M., Christodoulou, J., Wilson, M. R., and Dobson, C. M. (2005) Heat shock protein 70 inhibits  $\alpha$ -synuclein fibril formation via preferential binding to prefibrillar species. *J. Biol. Chem.* 280, 14733–14740.
- Schanda, P., and Brutscher, B. (2005) Very fast two-dimensional NMR spectroscopy for real-time investigation of dynamic events in proteins on the time scale of seconds. *J. Am. Chem. Soc.* 127, 8014–8015.
- Hsu, S. D., Bertocini, C. W., and Dobson, C. M. (2009) Use of protonless NMR spectroscopy to alleviate the loss of information resulting from exchange-broadening. *J. Am. Chem. Soc.* 131, 7222–7223.
- Bermel, W., Bertini, I., Felli, I. C., Matzapetakis, M., Pierattelli, R., Theil, E. C., and Turano, P. (2007) A method for  $\text{C}\alpha$  direct-detection in protonless NMR. *J. Magn. Reson.* 188, 301–310.
- Wilkins, D. K., Grimshaw, S. B., Receveur, V., Dobson, C. M., Jones, J. A., and Smith, L. J. (1999) Hydrodynamic radii of native and denatured proteins measured by pulsed field gradient NMR techniques. *Biochemistry* 38, 16424–16431.
- Conway, K. A., Lee, S. J., Rochet, J. C., Ding, T. T., Harper, J. D., Williamson, R. E., and Lansbury, P. T. J. (2000) Accelerated oligomerization by Parkinson's disease linked  $\alpha$ -synuclein mutants. *Ann. N.Y. Acad. Sci.* 920, 42–45.
- Han, H., Weinreb, P. H., and Lansbury, P. T. J. (1995) The core Alzheimer's peptide NAC forms amyloid fibrils which seed and are seeded by  $\beta$ -amyloid: is NAC a common trigger or target in neurodegenerative disease? *Chem. Biol.* 2, 163–169.
- El-Agnaf, O. M. A., and Irvine, G. B. (2002) Aggregation and neurotoxicity of  $\alpha$ -synuclein and related peptides. *Biochem. Soc. Trans.* 30, 559–565.
- Hoyer, W., Cherny, D., Subramaniam, V., and Jovin, T. M. (2004) Impact of the acidic C-terminal region comprising amino acids 109–140 on  $\alpha$ -synuclein aggregation in vitro. *Biochemistry* 43, 16233–16242.
- Uversky, V. N., Li, J., and Fink, A. L. (2001) Trimethylamine-N-oxide-induced folding of  $\alpha$ -synuclein. *FEBS Lett.* 509, 31–35.
- Munishkina, L. A., Henriques, J., Uversky, V. N., and Fink, A. L. (2004) Role of protein-water interactions and electrostatics in  $\alpha$ -synuclein fibril formation. *Biochemistry* 43, 3289–3300.
- Barbosa, L. R. S., Itri, R., Caetano, W., de Sousa Neto, D., and Tabak, M. (2008) Self-assembling of phenothiazine compounds investigated by small-angle X-ray scattering and electron paramagnetic resonance spectroscopy. *J. Phys. Chem. B* 112, 4261–4269.
- Morar, A. S., Olteanu, A., Young, G. B., and Pielak, G. J. (2001) Solvent-induced collapse of  $\alpha$ -synuclein and acid-denatured cytochrome c. *Protein Sci.* 10, 2195–2199.
- Bertoncini, C. W., Rasia, R. M., Lamberto, G. R., Binolfi, A., Zweckstetter, M., Griesinger, C., and Fernandez, C. O. (2007) Structural characterization of the intrinsically unfolded protein  $\beta$ -synuclein, a natural negative regulator of  $\alpha$ -synuclein aggregation. *J. Mol. Biol.* 372, 708–722.
- Chanamai, R., and McClements, D. J. (2001) Isothermal titration calorimetry measurement of enthalpy changes in monodisperse oil-in-water emulsions undergoing depletion flocculation. *Colloids Surf. A* 181, 261–269.

44. Bijma, K., Engberts, J. B. F. N., Blandamer, M. J., Cullis, P. M., Last, P. M., Irlam, K., and Soldi, L. G. (1997) Classification of calorimetric titration plots for alkytrimethylammonium and alkyipyridinium cationic surfactants in aqueous solutions. *J. Chem. Soc. Faraday Trans. 93*, 1579–1584.
45. Kim, Y., Randolph, T. W., Manning, M. C., Stevens, F. J., and Carpenter, J. F. (2003) Congo red populates partially unfolded states of an amyloidogenic protein to enhance aggregation and amyloid fibril formation. *J. Biol. Chem.* 278, 10842–10850.
46. Uversky, V. N., Li, J., Souillac, P., Millett, I. S., Doniach, S., Jakes, R., Goedert, M., and Fink, A. L. (2002) Biophysical properties of the synucleins and their propensities to fibrillate: inhibition of  $\alpha$ -synuclein assembly by  $\beta$ - and  $\gamma$ -synucleins. *J. Biol. Chem.* 277, 11970–11978.
47. Zhu, M., Rajamani, S., Kaylor, J., Han, S., Zhou, F., and Fink, A. L. (2004) The flavonoid baicalein inhibits fibrillation of  $\alpha$ -synuclein and disaggregates existing fibrils. *J. Biol. Chem.* 279, 26846–26857.
48. Pandey, N., Strider, J., Nolan, W. C., Yan, S. X., and Galvin, J. E. (2008) Curcumin inhibits aggregation of  $\alpha$ -synuclein. *Acta Neuropathol.* 115, 479–489.
49. Madine, J., Doig, A. J., and Middleton, D. A. (2008) Design of an N-methylated peptide inhibitor of  $\alpha$ -synuclein aggregation guided by solid-state NMR. *J. Am. Chem. Soc.* 130, 7873–7881.
50. Li, J., Zhu, M., Rajamani, S., Uversky, V. N., and Fink, A. L. (2004) Rifampicin inhibits  $\alpha$ -synuclein fibrillation and disaggregates fibrils. *Chem. Biol.* 11, 1513–1521.
51. El-Agnaf, O. M. A., Paleologou, K. E., Greer, B., Abogre, A. M., King, J. E., Salem, S. A., Fullwood, N. J., Benson, F. E., Hewitt, R., Ford, K. J., Martin, F. L., Harriott, P., Cookson, M. R., and Allsop, D. (2004) A strategy for designing inhibitors of  $\alpha$ -synuclein aggregation and toxicity as a novel treatment for Parkinson's disease and related disorders. *FASEB J.* 18, 1315–1317.
52. Conway, K. A., Rochet, J. C., Bieganski, R. M., and Lansbury, P. T. J. (2001) Kinetic stabilization of the  $\alpha$ -synuclein protofibril by a dopamine- $\alpha$ -synuclein adduct. *Science* 294, 1346–1349.
53. Stopa, B., Rybarska, J., Drozd, A., Konieczny, L., Król, M., Lisowski, M., Piekarska, B., Roterman, I., Spólnik, P., and Zemanek, G. (2006) Albumin binds self-assembling dyes as specific polymolecular ligands. *Int. J. Biol. Macromol.* 40, 1–8.
54. Kuciel, R., and Mazurkiewicz, A. (1997) Molten globule as an intermediate on the human prostatic phosphatase folding pathway. *Acta Biochim. Pol.* 44, 645–657.
55. Necula, M., Chirita, C. N., and Kuret, J. (2003) Rapid anionic micelle-mediated  $\alpha$ -synuclein fibrillization *in vitro*. *J. Biol. Chem.* 278, 46674–46680.
56. Ghuman, J., Zunszain, P. A., Petitpas, I., Bhattacharya, A. A., Otagiri, M., and Curry, S. (2005) Structural basis of the drug-binding specificity of human serum albumin. *J. Mol. Biol.* 353, 38–52.
57. Zhu, M., Souillac, P. O., Ionescu-Zanetti, C., Carter, S. A., and Fink, A. L. (2002) Surface-catalyzed amyloid fibril formation. *J. Biol. Chem.* 277, 50914–50922.
58. Rudyk, H., Vasiljevic, S., Hennion, R. M., Birkett, C. R., Hope, J., and Gilbert, I. H. (2000) Screening congo red and its analogues for their ability to prevent the formation of Prp-res in scrapie-infected cells. *J. Gen. Virol.* 81, 1155–1164.
59. Crowther, D. C., Kinghorn, K. J., Miranda, E., Page, R., Curry, J. A., Duthie, F. A. I., Gubb, D. C., and Lomas, D. A. (2005) Intra-neuronal  $\alpha\beta$ , non-amyloid aggregates and neurodegeneration in a drosophila model of Alzheimer's disease. *Neuroscience* 132, 123–135.
60. Frenkel, Y. V., Clark, A. D. J., Das, K., Wang, Y., Lewi, P. J., Janssen, P. A. J., and Arnold, E. (2005) Concentration and pH dependent aggregation of hydrophobic drug molecules and relevance to oral bioavailability. *J. Med. Chem.* 48, 1974–1983.